Acta Mech 223, 2065–2074 (2012)
DOI 10.1007/s00707-012-0682-4

U. Güven

A more general investigation for the longitudinal stress waves in microrods with initial stress

Received: 15 December 2011 / Revised: 20 April 2012 / Published online: 24 June 2012

Abstract In the present work, the propagation of longitudinal stress waves along a nanoscale bar with initial stress is investigated by using a unified nonlocal model with two length scale parameters. In principle, the analysis of wave motion is based on Love rod theory including the effects of lateral deformation. However, here are not ignored the contribution of shear stress components due to lateral deformations in the calculation of total elastic strain energy. By applying Hamilton's principle, the explicit general solution is obtained, and comparative results containing the different effects are presented and discussed.

1 Introduction

The propagation of longitudinal stress waves in micro/nanostructural elements has been the subject of numerous recent studies. When the classical continuum theories are applied to the analysis of these small structures, they are found to be inadequate in the explanation of the size-dependent behavior. Therefore, the wave propagation analysis in different structural elements (e.g. beam, rod, bar, plate, shell) having extremely small overall dimensions can be investigated with the nonlocal continuum theories, which reflect the microstructural features. The longitudinal stress waves in an infinite circular cylindrical rod made of an isotropic nonlocal material were investigated [1]. The longitudinal wave propagation in a one-dimensional nanorod was studied [2] using the Laplace transform technique under time-harmonic conditions. A detailed study on the dispersion of longitudinal waves in single-walled armchair carbon nanotubes was presented in [3]. The group velocities of longitudinal and flexural wave propagations in single- and multi-walled carbon nanotubes were studied [4] in the frame of continuum mechanics. A unified model including both the classical gradient model and Eringen's integral model was developed [5] for the wave propagation in a nonlocal elastic material. The effects of initial axial stress on wave propagation in SWNTs and DWNTs was investigated [6] using a generalized nonlocal beam model. The transverse wave characteristics of carbon nanotubes was studied [7] using a generalized gradient elasticity beam model. A nonlocal Euler–Bernoulli bar model was developed [8] for analyzing the ultrasonic wave propagation in nanorods. The axial wave propagation of a double nanorod system was investigated [9] using Eringen's nonlocal elasticity theory. A nonlocal continuum model including the lateral inertia effect, but without the initial stress effect, was developed [10] for analyzing the ultrasonic wave propagation in nanorods. In [11], Eringen's nonlocal elasticity theory was used to model the dispersion characteristics of ultrasonic waves in a nanorod. A nonlocal Euler–Bernoulli bar model was developed [12] for constructing a spectral finite element dynamic stiffness matrix of nanorods. Furthermore, a detailed study on nonlocal

Dedicated to Herrn Professor Udo Gamer on the occasion of his 75th birthday.

U. Güven (✉)
School of Mechanical Engineering, Yildiz Technical University, Besiktas, 34349 Istanbul, Turkey
E-mail: uguven@yildiz.edu.tr
Tel.: +90-0212-3832823
Fax: +90-0212-2616659

torsional vibration of nanorods can be found in [13]. The small-scale effect on the axial vibration of clamped–clamped and clamped-free nanorods was studied in [14]. The size-dependent free vibration of nanotubes with surface effects was investigated [15] using Love's continuum model for longitudinal wave propagation. A nonlocal elasticity solution for the longitudinal stress waves of bars was presented [16] based on the modified couple stress theory [17], love rod model [18] and Kecs approach [19]. In the meantime, it should be mentioned that for the nanoscale wave propagation, some interesting works that contain new dispersion and spectrum relations can be found in [20–22].

The initial stresses occurring in micro- or nanostructures, particularly due to the different manufacturing processes, are more important compared to other conventional structures, as mentioned in [23]. Current literature shows that the initial stress effects on the nanoscale wave propagation mostly have been studied using the Bernoulli–Euler rod model. Therefore, in this work, the longitudinal stress waves for micro- or nanobars are investigated under the initial stress (compressive or tensile) effect, in a more general frame. In the present analysis, a unified nonlocal elasticity model is used, and the lateral deformation and the shear strain effects are also considered. The aim of this work is to investigate more realistically the longitudinal stress waves under the existing initial stress.

2 Basic equations and differential equations of motion

According to the basic hypotheses of the Love approach, the displacement field is expressed as

$$u = u\,(x,t)\,, \quad v = -\nu y \frac{\partial u}{\partial x} \quad \text{and} \quad w = -\nu z \frac{\partial u}{\partial x}, \tag{1}$$

where u, v and w are the x, y and z components of the displacement vector, respectively, and ν is the Poisson's ratio. The x axis is taken in the longitudinal direction of the microbar; y and z are the axes at the geometrical centre of the cross-section.

For the displacement field specified by Eq. (1), the strains and stresses are conventionally obtained as

$$\begin{aligned} &\varepsilon_{\mathrm{x}} = \frac{\partial u}{\partial x}, \quad \varepsilon_{\mathrm{y}} = \frac{\partial v}{\partial y} = -\nu \frac{\partial u}{\partial x}, \quad \varepsilon_{\mathrm{z}} = \frac{\partial w}{\partial z} = -\nu \frac{\partial u}{\partial x}, \quad \gamma_{xy} = \frac{\partial u}{\partial y} + \frac{\partial v}{\partial x} = -\nu y \frac{\partial^2 u}{\partial x^2}, \\ &\gamma_{xz} = 2\varepsilon_{xz} = \frac{\partial w}{\partial z} + \frac{\partial u}{\partial z} = -\nu z \frac{\partial^2 u}{\partial x^2}, \quad \gamma_{yz} = 2\varepsilon_{yz} = \frac{\partial w}{\partial y} + \frac{\partial v}{\partial z} = 0, \end{aligned} \tag{2}$$

$$\sigma_{xx} = E\varepsilon_x, \quad \sigma_{yy} = \sigma_{zz} = 0, \quad \tau_{xy} = -\frac{E}{2(1+v)} v y \frac{\partial^2 u}{\partial x^2}, \quad \tau_{xz} = -\frac{E}{2(1+v)} v z \frac{\partial^2 u}{\partial x^2}, \quad \tau_{yz} = 0, \tag{3}$$

where ε_x, ε_y and ε_z are the normal strains, γ_{xy}, γ_{xz} and γ_{yz} are the shear strains, σ_{xx}, σ_{yy} and σ_{zz} are the normal stresses, τ_{xy}, τ_{xz} and τ_{yz} are the shear stresses and E is the elasticity modulus.

The differential equations of motion, taking into account the presence of initial stress, can be expressed as follows [24,25]:

$$\frac{\partial \sigma_{xx}}{\partial x} + \frac{\partial \tau_{xy}}{\partial y} + \frac{\partial \tau_{xz}}{\partial z} - \frac{N_0}{A}\frac{\partial^2 u}{\partial x^2} = \rho\frac{\partial^2 u}{\partial t^2}, \tag{4}$$

$$\frac{\partial \tau_{yx}}{\partial x} + \frac{\partial \sigma_{yy}}{\partial y} + \frac{\partial \tau_{yz}}{\partial z} - \frac{N_0}{A}\frac{\partial^2 v}{\partial x^2} = \rho\frac{\partial^2 v}{\partial t^2}, \tag{5}$$

$$\frac{\partial \tau_{zx}}{\partial x} + \frac{\partial \tau_{zy}}{\partial y} + \frac{\partial \sigma_{zz}}{\partial z} - \frac{N_0}{A}\frac{\partial^2 w}{\partial x^2} = \rho\frac{\partial^2 w}{\partial t^2}, \tag{6}$$

where N_0 is the axial initial force and A is the perpendicular cross-sectional area of the bar.

3 Unified nonlocal model and general solution

The unified nonlocal model used in the present analysis is based on combining the nonlocal integral model of Eringen [26] and the gradient elasticity model [27–30]. This unified model [5,6 and 30] has been proposed as

$$\left(1 - l_m \nabla^2\right)\sigma_{ij} = \left(1 - l_s \nabla^2\right)\left(\lambda\delta_{ij}\,\varepsilon_{kk} + 2G\,\varepsilon_{ij}\right), \tag{7}$$

where l_m and l_s are the material constants in the nonlocal integral model and in the gradient elasticity model, respectively. λ and G are Lamé constants, ∇^2 $(=\frac{\partial^2}{\partial x^2}+\frac{\partial^2}{\partial y^2}+\frac{\partial^2}{\partial z^2})$ is the Laplacian operator and δ_{ij} denotes the Kronecker delta.

Using Eqs. (4)–(7), and after a few simple derivative operations, the existing stress components are obtained:

$$\sigma_{xx}=(1+2\nu)\,l_m^2\left(\frac{N_0}{A}\frac{\partial^3 u}{\partial x^3}+\rho\,\frac{\partial^3 u}{\partial x\partial t^2}\right)+E\left(\frac{\partial u}{\partial x}-l_\mathrm{s}^2\frac{\partial^3 u}{\partial x^3}\right), \tag{8}$$

$$\tau_{xy}=-\nu y l_m^2\left(\frac{N_0}{A}\frac{\partial^4 u}{\partial x^4}+\rho\,\frac{\partial^4 u}{\partial x^2\partial t^2}\right)+\frac{E\nu y}{2\,(1+\nu)}\left(l_\mathrm{s}^2\frac{\partial^4 u}{\partial x^4}-\frac{\partial^2 u}{\partial x^2}\right), \tag{9}$$

$$\tau_{xz}=-\nu z l_m^2\left(\frac{N_0}{A}\frac{\partial^4 u}{\partial x^4}+\rho\,\frac{\partial^4 u}{\partial x^2\partial t^2}\right)+\frac{E\nu z}{2\,(1+\nu)}\left(l_\mathrm{s}^2\frac{\partial^4 u}{\partial x^4}-\frac{\partial^2 u}{\partial x^2}\right), \tag{10}$$

In the present analysis, the governing equation of longitudinal wave motion is deduced from Hamilton's principle. Here, the total elastic strain energy including also the contribution of shear stress components is expressed as in [19]:

$$U=\frac{1}{2}\int\int\int\left(\sigma_{xx}\varepsilon_{xx}+\tau_{xy}\gamma_{xy}+\tau_{xz}\gamma_{xz}\right)\mathrm{d}V. \tag{11}$$

The kinetic energy T is given by

$$T=\frac{1}{2}\,\rho\int\int\int\left(\dot{u}^2+\dot{v}^2+\dot{w}^2\right)\mathrm{d}V. \tag{12}$$

The potential energy V is given by

$$V=-\frac{1}{2}\int_0^{\mathrm{L}} N_0\left(\frac{\partial u}{\partial x}\right)^2\mathrm{d}x. \tag{13}$$

By putting Eqs. (8–10) into Eq. (11), the total elastic strain energy expression becomes

$$\begin{aligned}U=\frac{1}{2}\int_0^{\mathrm{L}}\Bigg\{&(1+2\nu)\,l_m^2\left(N_0\frac{\partial u}{\partial x}\frac{\partial^3 u}{\partial x^3}+\rho\,A\frac{\partial u}{\partial x}\frac{\partial^3 u}{\partial x\partial t^2}\right)+EA\left(\frac{\partial u}{\partial x}\right)^2-EAl_\mathrm{s}^2\frac{\partial u}{\partial x}\frac{\partial^3 u}{\partial x^3}\\&+l_m^2\nu^2 I_\mathrm{p}\left(\frac{N_0}{A}\frac{\partial^2 u}{\partial x^2}\frac{\partial^4 u}{\partial x^4}+\rho\,\frac{\partial^2 u}{\partial x^2}\frac{\partial^4 u}{\partial x^2\partial t^2}\right)-\frac{E\nu^2 I_\mathrm{p}}{2\,(1+\nu)}\left[l_\mathrm{s}^2\frac{\partial^2 u}{\partial x^2}\frac{\partial^4 u}{\partial x^4}-\left(\frac{\partial^2 u}{\partial x^2}\right)^2\right]\Bigg\}\mathrm{d}x,\end{aligned} \tag{14}$$

where I_p denotes the second polar moment.When considered the displacement field (1), the kinetic energy expression becomes

$$T=\frac{1}{2}\int_0^{\mathrm{L}}\left[\rho\,A\left(\frac{\partial u}{\partial t}\right)^2+\rho\,\nu^2 I_\mathrm{p}\left(\frac{\partial^2 u}{\partial x\partial t}\right)^2\right]\mathrm{d}x. \tag{15}$$

By applying Hamilton's principle (the Lagrangian function is $L=T-U-V$), the governing equation of motion is obtained as follows:

$$\begin{aligned}&-\frac{\rho}{E}\frac{\partial^2 u}{\partial t^2}+\left(1-\frac{N_0}{AE}\right)\frac{\partial^2 u}{\partial x^2}+(1+2\nu)\,l_m^2\left(\frac{N_0}{AE}\frac{\partial^4 u}{\partial x^4}+\frac{\rho}{E}\frac{\partial^4 u}{\partial x^2\partial t^2}\right)\\&-l_\mathrm{s}^2\frac{\partial^4 u}{\partial x^4}-\nu^2 r_0^2 l_m^2\left(\frac{N_0}{AE}\frac{\partial^6 u}{\partial x^6}+\frac{\rho}{E}\frac{\partial^6 u}{\partial x^4\partial t^2}\right)\\&-\frac{\nu^2 r_0^2}{2\,(1+\nu)}\frac{\partial^4 u}{\partial x^4}+l_\mathrm{s}^2\frac{\nu^2 r_0^2}{2\,(1+\nu)}\frac{\partial^6 u}{\partial x^6}+\frac{\rho}{E}\nu^2 r_0^2\frac{\partial^4 u}{\partial x^2\partial t^2}=0.\end{aligned} \tag{16}$$

Associated boundary conditions are

$$\left[(N_o - EA)\frac{\partial u}{\partial x} + \left(EAl_s^2 + \frac{E\nu^2 I_p}{2(1+\nu)} - l_m^2(1+2\nu)N_o\right)\frac{\partial^3 u}{\partial x^3} + \left(l_m^2\nu^2 I_p\frac{N_o}{A} - \frac{l_s^2 E\nu^2 I_p}{2(1+\nu)}\right)\frac{\partial^5 u}{\partial x^5} - \left(\rho\nu^2 I_p + l_m^2(1+2\nu)\rho A\right)\frac{\partial^3 u}{\partial x\partial t^2} + l_m^2\rho\nu^2 I_p\frac{\partial^5 u}{\partial x^3\partial t^2}\right]|\delta u|_0^L = 0, \tag{17.1}$$

$$\left[\frac{1}{2}\left(l_m^2(1+2\nu)N_o - l_s^2 EA - \frac{E\nu^2 I_p}{2(1+\nu)}\right)\frac{\partial^2 u}{\partial x^2} + \left(\frac{l_s^2 E\nu^2 I_p}{2(1+\nu)} - l_m^2\nu^2 I_p\frac{N_o}{A}\right)\frac{\partial^4 u}{\partial x^4} - l_m^2\nu^2 I_p\rho\frac{\partial^4 u}{\partial x^2\partial t^2}\right], \quad \left|\delta u'\right|_0^L = 0, \tag{17.2}$$

$$\left[\frac{1}{2}\left(l_s^2 EA - l_m^2(1+2\nu)N_o\right)\frac{\partial u}{\partial x} + \frac{1}{2}\left(l_m^2\nu^2 I_p\frac{N_o}{A} - \frac{l_s^2 E\nu^2 I_p}{2(1+\nu)}\right)\frac{\partial^3 u}{\partial x^3}\right]\left|\delta u''\right|_0^L = 0, \tag{17.3}$$

$$\left[\frac{1}{2}\left(\frac{l_s^2 E\nu^2 I_p}{2(1+\nu)} - l_m^2\nu^2 I_p\frac{N_o}{A}\right)\frac{\partial^2 u}{\partial x^2}\right]\left|\delta u'''\right|_0^L = 0. \tag{17.4}$$

In this study, a harmonic longitudinal wave propagating along the axial direction is assumed, and therefore its propagation can be expressed in the complex form as

$$u = \tilde{U}e^{ik(x-ct)}, \tag{18}$$

where k denotes the wave number, c is the phase velocity and $\tilde{U}$ is the wave amplitude.

Substituting Eq. (18) into the governing equation (16), the corresponding general solution for the phase velocity is obtained in dimensionless form as

$$c^* = \sqrt{\frac{1-\gamma+\left(\frac{\nu^2 r_0^2 k^2}{2(1+\nu)}\right) - \gamma k^2 l_m^2\left[(1+2\nu)+\nu^2 r_0^2 k^2\right] + l_s^2 k^2\left[1+\frac{\nu^2 r_0^2 k^2}{2(1+\nu)}\right]}{1+\nu^2 r_0^2 k^2 + k^2 l_m^2\left[(1+2\nu)+\nu^2 r_0^2 k^2\right]}}, \tag{19}$$

where $c^* = \frac{c}{c_0}$, $c_0 = \sqrt{\frac{E}{\rho}}$, $r_0 = \sqrt{\frac{I_p}{A}}$ and $\gamma = \frac{N_0}{AE}$. For a rod, the gyration radius r_0 is given by $(a/\sqrt{2})$, where a is the radius of rod.

The angular frequency is given by

$$\omega = c_o\sqrt{\frac{(1-\gamma)k^2+\left(\frac{\nu^2 r_0^2 k^4}{2(1+\nu)}\right) - \gamma k^4 l_m^2\left[(1+2\nu)+\nu^2 r_0^2 k^2\right] + l_s^2 k^4\left[1+\frac{\nu^2 r_0^2 k^2}{2(1+\nu)}\right]}{1+\nu^2 r_0^2 k^2 + k^2 l_m^2\left[(1+2\nu)+\nu^2 r_0^2 k^2\right]}}. \tag{20}$$

The group velocity ($c_g = \frac{\partial\omega}{\partial k}$) can be obtained as

$$c_g = c_o\frac{1-\gamma+2a_1k^2+\left[3a_2+2a_1b_1-b_2(1-\gamma)\right]k^4+2a_2b_1k^6+a_2b_2k^8}{\left(1-\gamma+a_1k^2+a_2k^4\right)^{1/2}\left(1+b_1k^2+b_2k^4\right)^{3/2}}, \tag{21}$$

where

$$a_1 = \frac{\nu^2 r_o^2}{2(1+\nu)} + l_s^2 - \gamma l_m^2(1+2\nu), \quad a_2 = l_s^2\frac{\nu^2 r_o^2}{2(1+\nu)} - \gamma l_m^2\nu^2 r_o^2,$$
$$b_1 = \nu^2 r_o^2 + l_m^2(1+2\nu), \quad b_2 = l_m^2\nu^2 r_o^2.$$

4 Degenerate solutions and numerical results

In Figs. 1a, b, the dispersion curves based on the present nonlocal elasticity model including the lateral deformation and shear strain effects for the rod with the initial stress are compared with those of the rod without initial stress, for $\gamma = -0.05$ and $\gamma = 0.05$, respectively, where $m = l_s/l_m, lk$ is the dimensionless wave number, c^* denotes the dimensionless phase velocity for the initial stress case, and $c^*(\gamma = 0)$ denotes the dimensionless phase velocity for the initially stress—free state. The length scale parameters that are related to the microstructure can be estimated from molecular dynamics or molecular mechanics simulations and with the nonlocal theory. Eringen due to the different considerations proposed the values of l_m as $0.39d$ and $0.31d$ [26], where d denotes the distance between the atoms. The value of l_m was adopted as $0.39d$, in [31], following Eringen. In [32], the same parameter was identified as $0.82d$. In [5], the optimal value of l_m was identified as $0.218d$. The other length scale parameter l_s was identified in [30] as $d/\sqrt{12}$, also the same value was adopted in [33]. In [34], it was reported that the length scale parameter l_m should be less than 2 nm. Different values of the nonlocal length scale parameters available in literature also can be found in [35]. Although no sufficient information for the values of length scale parameters, they were taken into account to be the same order of the carbon–carbon bond length, as in [6]. Since the accurate values of the length scale parameters are not yet defined sufficiently, and furthermore, considering that they can take different values for different cases (e.g. crystal structures, working conditions), the ratio $m(=l_s/l_m)$ was taken as the variable in numerical calculations. In addition,the length scale parameter for the simple comparison aim is chosen as $l_m = l = a/\sqrt{96}$, and Poisson's ratio ν is taken as 1/3. Again, for the simplicity, the parameter l was expressed depending on of the rod radius a. Figures 1a, b show that the effect of initial stress (tensile or compression) on the dispersion curves is very unimportant for values of the scale length ratio $m > 1$.

By putting $l_m = l_s = 0$ in Eq. (19), the generalized local solution is obtained as

$$c^* = \sqrt{\frac{1 - \gamma + \left(\frac{\nu^2 r_0^2 k^2}{2(1+\nu)}\right)}{1 + \nu^2 r_0^2 k^2}}. \tag{22}$$

The above local solution (22) may be regarded as generalized Kecs solution [19] for the rod with initial stress.

On other hand, two important limit cases can be obtained from the general solution. Firstly, for short wavelengths (i.e. $k \to \infty$), the general dispersion relation (19) is reduced to the following form:

$$c^* = \sqrt{\left(\frac{l_s}{l_m}\right)^2 \frac{1}{2(1+\nu)} - \gamma}. \tag{23}$$

Equation (23) shows that for shorts wavelengths, the general dispersion relation derived here including lateral deformations and shear strains effects is not affected by the radius of the rod. It is clear that short waves will exist for dimensionless initial loading parameter $\gamma < 0$ (i.e. tensile loading). On the contrary, for dimensionless

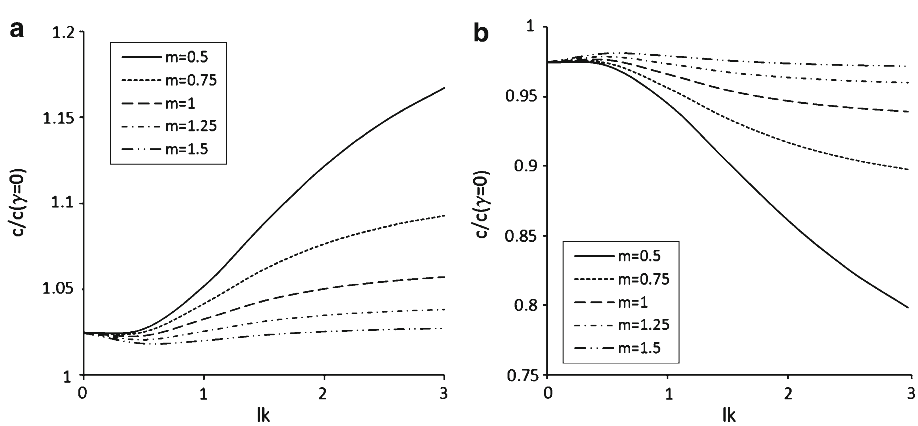

Fig. 1 Comparison of phase velocities based on the present solution via the initial stress presence, against the dimensionless wave number, for the different values of the material length scale ratio m: **a** $\gamma = -0.05$, **b** $\gamma = 0.05$

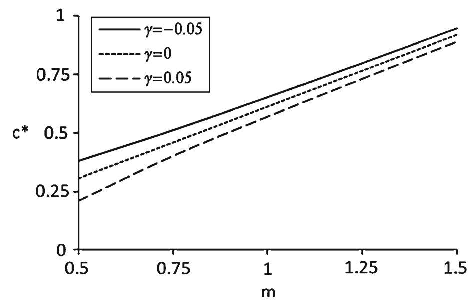

Fig. 2 Variation of the phase velocity based on the present solution in the case of short wave, against the material length scale ratio m, for $\gamma = -0.05, 0, 0.05$

initial loading parameter $\gamma > 0$ (i.e. compressive loading), the short waves will exist as long as this inequality is provided: $\gamma < \left(\frac{l_s}{l_m}\right)^2 \frac{1}{2(1+\nu)}$. It should be noticed that in the particular case $l_s = l_m$, scale effect is lost, and thus, the solution will be obtained in terms of ν and γ. Furthermore, it is also seen that the phase velocity is independent of the scale effect for $l_s = 0$ (i.e. Eringen'smodel), and therefore a nonlocal solution cannot be obtained for short waves. In addition, it must be also noticed that the local method gives a solution without Poisson's ratio only in terms of γ, and for the rod without the initial stress a solution cannot be obtained. Figure 2 shows that by increasing the parameter m, the phase velocity increases always (i.e. with initial tensile stress, initial compression stress and without initial stress cases).

Secondly, for long wavelengths (i.e. $k \to 0$), the general dispersion relation (19) is reduced to the following form:

$$c^* = \sqrt{1-\gamma}. \tag{24}$$

Equation (24) shows that for long wave lengths, generally both the local and nonlocal dispersion expressions presented here will be identical.

When ignoring the contribution of the shear stress components in the calculation of the total elastic strain energy, the governing equation of motion (16) is reduced to the following form:

$$\begin{aligned} &-\frac{1}{c_0^2}\frac{\partial^2 u}{\partial t^2} + \frac{\partial^2 u}{\partial x^2} - \frac{N_0}{AE}\frac{\partial^2 u}{\partial x^2} + \frac{1}{c_0^2}\nu^2 r_0^2 \frac{\partial^4 u}{\partial x^2 \partial t^2} \\ &+ l_m^2\left(\frac{N_0}{AE}\frac{\partial^4 u}{\partial x^4} + \frac{1}{c_0^2}\frac{\partial^4 u}{\partial x^2 \partial t^2} - \nu^2 r_0^2 \frac{N_0}{AE}\frac{\partial^6 u}{\partial x^6} - \frac{1}{c_0^2}\nu^2 r_0^2 \frac{\partial^6 u}{\partial x^4 \partial t^2}\right) - l_s^2 \frac{\partial^4 u}{\partial x^4} = 0, \end{aligned} \tag{25}$$

and the dispersion relation (19) is re-obtained in the following reduced form:

$$c_L^* = \sqrt{\frac{1-\gamma-\gamma k^2 l_m^2 (1+\nu^2 k^2 r_0^2) + k^2 l_s^2}{1+\nu^2 k^2 r_0^2 + k^2 l_m^2\left(1+\nu^2 k^2 r_0^2\right)}}. \tag{26}$$

The above dispersion relation may be regarded as the generalized Love dispersion relation and is denoted by c_L^*. By setting $\nu = 0$ in the above equation (26), the previous solution [6] is obtained as follows:

$$c^* = \sqrt{\frac{1+l_s^2 k^2}{1+l_m^2 k^2} - \gamma}, \tag{27}$$

and when $\nu = \gamma = l_s = 0$, the other previous solution [8] is obtained.

In Figs. 3a, b, the dispersion curves based on the generalized nonlocal Love model for the rod with the initial stress are compared to those of the rod without the initial stress; for $\gamma = -0.05$ and, $\gamma = 0.05$, respectively, c_L^* denotes the dimensionless phase velocity for the initial stress case, and c_L^* ($\gamma = 0$) denotes the dimensionless phase velocity without the initial stress case. Figure 3a shows that the initial stress effect decreases the value of the phase velocity with increasing scale parameters ratio $m(= l_s/l_m)$, in the tensile initial axial loading case. However, Fig. 3b shows that for the compressive initial axial load case, this effect is

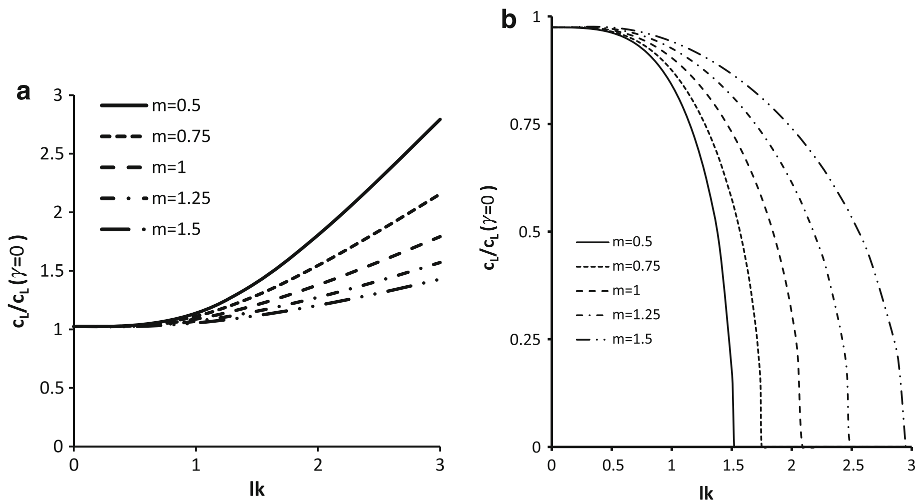

Fig. 3 Comparison of phase velocities based on the generalized Love rod solution via the initial stress presence, against the dimensionless wave number, for the different values of the material length scale ratio m: **a** $\gamma = -0.05$, **b** $\gamma = 0.05$

very different. It can be seen from Eq. (26) that as the dimensionless wave number lk exceeds the critical value, the phase velocity becomes imaginary. As stated clearly in [36,37], here the angular frequency (see Eq. (28)) also becomes imaginary, which corresponds to the exponential instability. In this case, the width of stationary zone is determined by the critical wave length $\lambda_{\text{crit}} = 2\pi/k_{\text{crit}}$. In Fig. 3b, the critical dimensionless wave numbers $(lk)_{\text{crit}}$ for $m(l_s/l_m) = 0.5$, 0.75, 1, 1.25 and 1.5 are obtained, respectively, as: 1.51636, 1.75469, 2.09352, 2.49851 and 2.94301.

When comparing Figs. 1 and 3, for the tensile initial axial load case, it can be concluded that the shear strain effect for the phase velocity is significant for the values of the scale length ratio $m\ (= l_s/l_m)$ relatively small (e.g. $m = 0.5$), and in particularly for high wave numbers. A comparison between Figs. 1b and 3b shows that the present general model under compressive axial load has not encountered any critical wave number, in the same range, contrary to the nonlocal Love model. This result is probably due to the negligence of the shear strain effect.

For short wavelengths (i.e. $k \to \infty$), the Love dispersion relation (26) is reduced to the following form:

$$c^* = \sqrt{-\gamma}. \tag{28}$$

Equation (28) shows clearly that the short waves only will exist for dimensionless initial loading parameter $\gamma < 0$ (i.e. tensile loading), and contrary to the general solution (i.e. Eq. (23)), the result does not depend on the scale parameters.

The angular frequency ω_L becomes

$$\omega_L = c_{\text{o}}\sqrt{\frac{(1-\gamma)\,k^2 + -\gamma k^4 \mathrm{l}_m^2\left[1+\nu^2 r_0^2 k^2\right] + \mathrm{l}_s^2 k^4}{1+\nu^2 r_0^2 k^2 + k^2 \mathrm{l}_m^2\left[1+\nu^2 r_0^2 k^2\right]}}. \tag{29}$$

The tensile initial axial load effect on the angular frequency is compared for the present general nonlocal, and the nonlocal Love models, in Figs. 4a, b. γ is taken as 0.05, where $\bar{\omega}$ is the dimensionless angular frequency and is defined as $\bar{\omega} = \omega a/c_o$.The comparison shows that this effect is crucial for the nonlocal Love model. In particular for high values of the wave number and small values of the materials parameters ratio $m\ (= l_s/l_m)$, this effect becomes more significant.

The group velocity c_{gL} is obtained as

$$c_{gL} = c_o \frac{(1-\gamma) + 2\left(m^2-\gamma\right) l^2k^2 + \left(2m^2l^2 + 2m^2\nu^2r_o^2 - 5\gamma\nu^2r_o^2\right) l^2k^4 - 2\gamma l^2k^6\nu^2r_o^2\left(l^2+\nu^2r_o^2\right) - \gamma l^4k^8\nu^4r_o^4}{\sqrt{\left[(1-\gamma) + \left(m^2-\gamma\right) l^2k^2 - \gamma l^2k^4\nu^2r_o^2\right]}\sqrt[3]{\left[1+\left(\nu^2r_o^2+l^2\right)k^2 + l^2k^4\nu^2r_o^2\right]}}, \tag{30}$$

where the subscript L denotes the Love rod model.

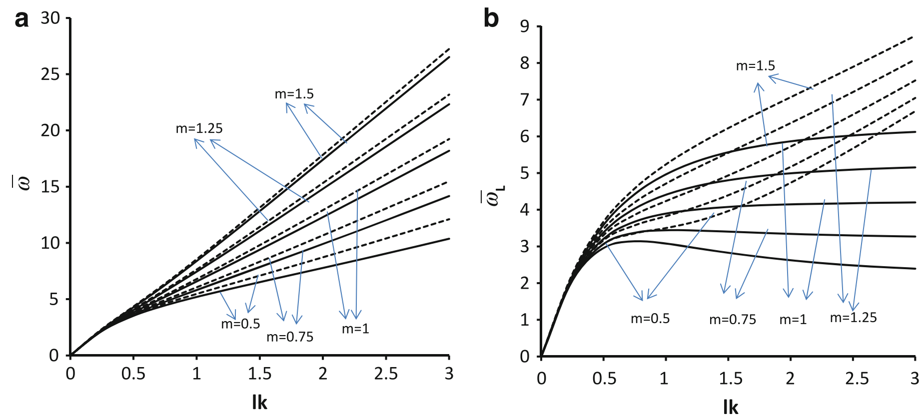

Fig. 4 Variations of the dimensionless angular frequencies against the dimensionless wave number **a** the present solution, **b** the nonlocal Love solution, for $\gamma = -0.05$ (*dashed line*) and $\gamma = 0$ (*solid line*)

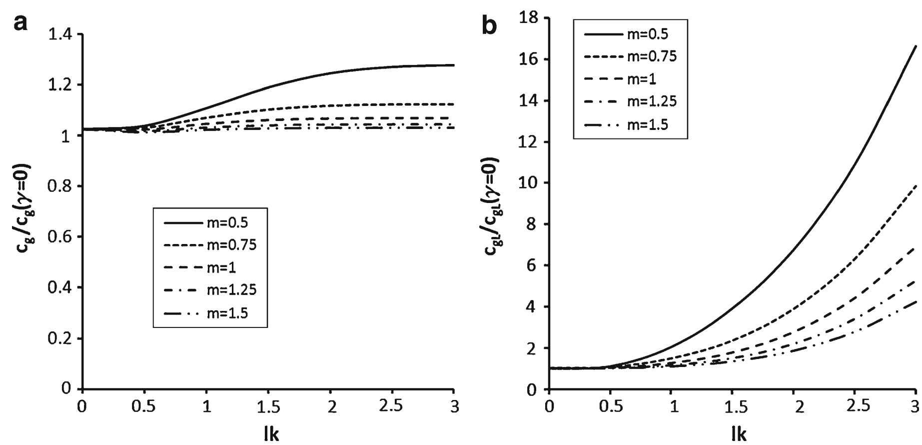

Fig. 5 Comparison of group velocities based on the present solution via the initial stress presence against the dimensionless wave number for the different values of the material length scale ratio m, and $\gamma = -0.05$ **a** the present solution, **b** the nonlocal Love solution

The tensile initial axial load effect on the group velocity is compared for the present general nonlocal and the nonlocal Love models in Figs. 5a, b. γ is taken as 0.05. It can be seen from Fig. 5a that with increasing parameter m, the tensile stress effect on the group velocity decreases significantly. In general, for small values of the dimensionless wave numbers $lk < 0.5$, and for high values of $lk > 2$, this effect becomes less important. Therefore, the obtained results from the current general nonlocal model show that the tensile initial stress effect on the group velocity is not significant in general. It can be seen from Fig. 5b that the tensile initial stress effect on the group velocity increases always, for values of $lk < 0.5$. It can be concluded that in the nonlocal Love model, this increase is more significant for small values of m and for high values of lk. The comparison shows that this effect is more significant for the nonlocal Love model.

In Figs. 6a, b are compared, for the tensile initial axial load and the compressive initial axial loads, respectively, the angular frequency variations versus the wave number, for the present general nonlocal model, the nonlocal Love model and the Born–Karman model. In numerical calculations, $m\ (= l_s/l_m) = 2/3$ was taken as in [6], and the rod radius a was chosen to be $3d$. Figures 6a, b show that the existing general nonlocal solution presented here is more compatible with the Born–Karman solution.

The Born–Karman expression is given by

$$\omega = \frac{2c_o}{d}\,\mathrm{Sin}\left(\frac{kd}{2}\right), \tag{31}$$

where d denotes the distance between the atoms.

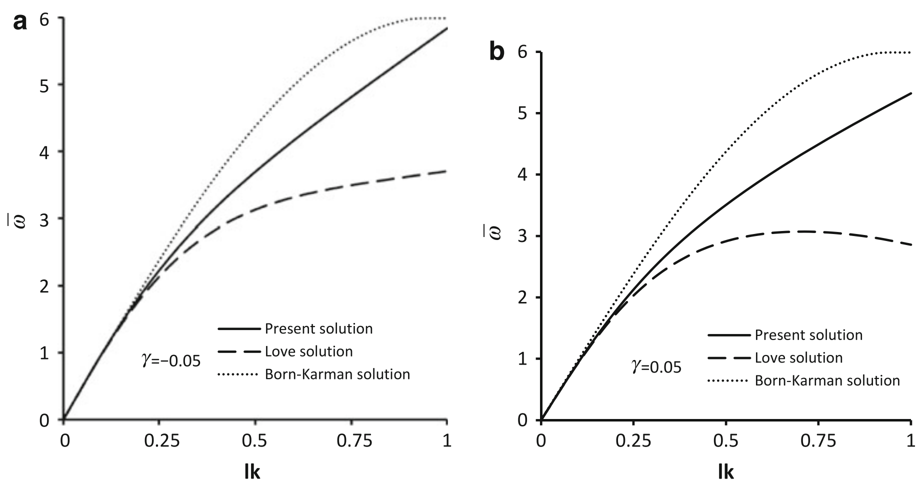

Fig. 6 Comparison of dimensionless angular frequencies for the present, the nonlocal Love and Born–Karman solutions **a** $\gamma = -0.05$, **b** $\gamma = 0.05$

5 Conclusions

In this work, the longitudinal stress waves in nanoscale bars under the initial stress effect are investigated in more detail by using a unified nonlocal elasticity model including both the integral and gradient models. The lateral deformation and shear strain effects on the phase velocity, the group velocity and angular frequency, are discussed under the initial stress presence. It is seen from the present work that, in particular, depending on the sign of the initial stress, the shear effect for the different cases can be significant. A general comparison between the present general nonlocal model and the nonlocal Love model shows that, in particular for the compressive initial stress, the results obtained from both models are too different to be significant. Furthermore, it is understood that the material length scale ratio has a crucial effect on the results. It can be concluded that the present unified nonlocal elasticity model gives more satisfactory and reasonable information regarding the characteristics of the longitudinal stress waves.

Acknowledgments The author is very grateful to Herrn Professor Franz Ziegler for leading the review process. The author also would like to thank the anonymous reviewers for their constructive comments and suggestions, which significantly improved this article.

References

1. Nowinski, J.L.: On a nonlocal theory of longitudinal waves in an elastic circular bar. Acta Mech. **52**, 189–200 (1984)
2. Manolis, G.D.: Some basic solutions for wave propagation in a rod exhibiting non-local elasticity. Eng. Anal. Bound. Elem. **24**, 503–508 (2000)
3. Wang, L., Hu, H., Guo, W.: Validation of the non-local elastic shell model for studying longitudinal waves in single-walled carbon nanotubes. Nanotechnology **17**, 1408–1415 (2006)
4. Wang, L., Guo, W., Hu, H.: Group velocity of wave propagation in carbon nanotubes. Proc. R. Soc. A **464**, 1423–1438 (2008)
5. Challamel, N., Rakotomanana, L., Marrec, L.L.: A dispersive wave equation using nonlocal elasticity. C.R. Mecanique **337**, 591–595 (2009)
6. Song, J., Shen, J., Li, X.F.: Effects on initial axial stress on waves propagating in carbon nanotubes using a generalized nonlocal model. Comput. Mater. Sci. **49**, 518–523 (2010)
7. Shen, J., Wu, J.X., Li, X.F., Lee, K.Y.: Flexural waves of carbon nanotubes based on generalized gradient elasticity. Phys. Status Solidi B **249**, 50–57 (2012)
8. Narendar, S., Gopalakrishnan, S.: Nonlocal scale effects on ultrasonic wave characteristics of nanorods. Physica E **42**, 1601–1604 (2010)
9. Narendar, S., Gopalakrishnan, S.: Axial wave propagation in coupled nanorod system with nonlocal small scale effects. Compos. Part B-Eng. **42**, 2013–2023 (2011)
10. Narendar, S.: Terahertz wave propagation in uniform nanorods: a nonlocal continuum mechanics formulation including the effect of lateral inertia. Physica E **43**, 1015–1020 (2011)
11. Narendar, S., Gopalakrishnan, S.: Ultrasonic wave characteristics of nanorods via nonlocal strain gradient models. J. Appl. Phys. **107**, 084312 (2010)

12. Narendar, S., Gopalakrishnan, S.: Spectral finite element formulation for nanorods via nonlocal continuum mechanics. ASME J. Appl. Mech. **78**, 061018 (2011)
13. Narendar, S.: Nonlocal torsional vibration of nanorods. J. Nanosci. Nanoeng. Appl. **1**, 36–51 (2011)
14. Aydogdu, M.: Axial vibration of the nanorods with the nonlocal continuum rod model. Physica E **41**, 861–864 (2009)
15. Assadi, A., Farshi, B.: Size—dependent longitudinal and transverse wave propagation in nanotubes with consideration of surface effects. Acta Mech. **222**, 27–39 (2011)
16. Güven, U.: The investigation of the nonlocal longitudinal stress waves with modified couple tress theory. Acta Mech. **221**, 321–325 (2011)
17. Yang, F., Chang, A.C.M., Lam, D.C.C., Tong, P.: Couple stress based strain gradient theory for elasticity. Int. J. Solids Struct. **39**, 2731–2743 (2002)
18. Love, A.E.H.: A Treatise on the Mathematical Theory of Elasticity. Dover Publications, New York (1944)
19. Kecs, W.W.: A generalized equation of longitudinal vibrations for elastic rods. The solution and uniqueness of a boundary-initial value problem. Eur. J. Mech. A/Solids **13**, 135–145 (1994)
20. Lim, C.V., Yang, Y.: New predictions of size—dependent nanoscale based on non-local elasticity for wave propagation in carbon nanotubes. J. Comput. Theor. Nanosci. **7**, 988–995 (2010)
21. Lim, C.V., Yang, Y.: Wave propagation in carbon nanotubes: nonlocal elasticity induced stiffness and velocity enhancement effects. J. Mech. Mater. Struct. **5**, 459–476 (2010)
22. Zhang, X., Sharma, P.: Size dependency of strain in arbitrary shaped anisotropic embedded quantum dots due to nonlocal dispersive effects. Phys. Rev. B. **72**, 195345 (2005)
23. Wang, C.M., Zhang, Y.Y., Kitipornchai, S.: Vibration of initially stressed micro-and nano-beams. Int. Struct. Stab. Dyn. **7**, 555–570 (2007)
24. Biot, M.A.: Mechanics of Incremental Deformations. Wiley, New York (1965)
25. Christensen, R.M.: Material instability for fibre composites. J. Appl. Mech. TASME **61**, 476–477 (1994)
26. Eringen, A.C.: Nonlocal Continuum Field Theories. Springer, New York (2002)
27. Lazar, M., Maugin, G.A.: Non-singular stress and strain field of dislocations and disclinations in first strain gradient elasticity. Int. J. Eng. Sci. **43**, 1157–1184 (2005)
28. Aifantis, E.C.: Uptadeon a class gradient theories. Mech. Mater. **35**, 259–280 (2003)
29. Askes, H., Aifantis, E.C.: Gradient elasticity and flexural wave dispersion in carbon nanotubes. Phys. Rev. B **80**, 195412 (2009)
30. Askes, H., Suiker, A.S.J., Sluys, L.J.: A classification of higher—order strain gradient models-linear analysis. Arch. Appl. Mech. **72**, 171–188 (2002)
31. Li, X.F., Wang, B.L., Mai, Y.W.: Effects of a surrounding elastic medium on flexural waves propagating in carbon nanotubes via nonlocal elasticity. J. Appl. Phys. **103**, 074309 (2009)
32. Zhang, Y.Q., Liu, G.R., Xie, X.Y.: Free transverse vibrations of double—walled carbon nanotubes using a theory of nonlocal elasticity. Phys. Rev. B **71**, 195404 (2005)
33. Wang, L., Hu, H.: Flexural wave propagation in single—walled carbon nanotubes. Phys. Rev. B **71**, 195412 (2005)
34. Wang, Y.Z., Li, F.M., Kishimoto, K.: Scale effects on flexural wave propagation in nano plate embedded in elastic matrix with initial stress. Appl. Phys. A **99**, 907–911 (2010)
35. Narendar, S., Gopalakrishnan, S.: Scale effects on buckling analysis of orthotropic nanoplates based on nonlocal two-variable refined plate theory. Acta Mech. **223**, 395–413 (2012)
36. Metrikine, A.V.: On causality of the gradient elasticity models. J. Sound Vib. **297**, 727–742 (2006)
37. Michelitsch, T.M., Gitman, I.M., Askes, H.: Critical wave lengths and instabilities in gradient—enriched continuum theories. Mech. Res. Commun. **34**, 515–521 (2007)